

SYNTHESIS AND CHARACTERIZATION OF MAGNESIUM-ZINC FERRITE PREPARED BY FLASH- COMBUSTION TECHNIQUE

Wai Khaing Moe¹, Phyu Phyu Khaing², Zin Bo Htut³,

Win Kyaw⁴ & Soe Soe Nwe⁵

Abstract

Magnesium-Zinc Ferrite, $Mg_{1-x}Zn_xFe_2O_4$ (where $x=0.50$) was prepared by flash-combustion technique. The sample was characterized by XRD, SEM and FTIR-spectroscopy to study the structural, microstructural and vibrational characteristics. XRD pattern revealed that the sample analogous to cubic structure with the lattice parameters $a=b=c=8.3512 \text{ \AA}$. The crystallite size was obtained as 47.96 nm and showed that the sample was the nanosized material. SEM micrograph showed that the grain shape of the sample was spherical with the grain sizes of $0.20 \mu\text{m} - 0.50\mu\text{m}$. Vibrational characteristics of tetrahedral site and octahedral site atoms were studied from the collected FTIR spectrum. Temperature dependent electrical conductivity and humidity sensitive electrical properties of the sample were observed for the applications of humidity sensing materials.

Keywords: Magnesium-Zinc Ferrite, Flash-Combustion, XRD, SEM, FTIR, humidity sensing materials

Introduction

Ferrites are still of interest as promising materials for many applications. For these reasons engineers and scientists are keenly interested in determining their characterization [Bhattacharjee, (2011)]. Since ferrites behave as low gap semiconductors and as insulators at low temperature, they have been used in number of technological applications [Gadkari, (2013)]. These applications include sensors, transformer core, microwave devices, magnetic and magneto-optic recording, data storage etc. [Maria1, (2013)].

Ferrite particles in nano scales can be produced by a large number of methods. These include soft chemical methods such as flash combustion

¹ Dr, Demonstrator, Department of Physics, Pyay University

² Dr, Assistant Lecturer, Department of Physics, Pyay University

³ Demonstrator, Department of Physics, Pyay University

⁴ Dr, Associate Professor, Department of Physics, Pyay University

⁵ Dr, Professor & HOD, Department of Physics, Pyay University

technique, co-precipitation method, sol gel synthesis, hydrothermal synthesis and mechano-synthesis approach of ball milling [Brito, (2010)] etc. Ferrites belong to a special class of magnetic material consisting of metal oxide and ferric oxide as their main compositions [Vagolu, (2013)]. The novel magnetic, electric and dielectric properties possessed by them have made ferrites more attractive to the current field of science and technology [Khot, (2011)]. These properties are largely dependent on chemical composition, method of synthesis, synthesis conditions, grain size and surface morphology.

This work preferred the Mg based ferrite from the two following reasons: (i) it is a slight porous ceramic and (ii) the stability of Mg^{2+} ions avoid the appearance of Fe^{2+} ions (essential require to obtain high resistivity). In the present work, Magnesium-Zinc ferrite, $Mg_{1-x}Zn_xFe_2O_4$ (where $x = 0.50$) was prepared by flash-combustion technique and their structural, microstructural and vibrational characteristics were studied by using XRD, SEM and FTIR methods. Temperature dependent electrical properties were also investigated. Furthermore, humidity sensitive electrical resistances, dc voltages and capacitances were investigated in the relative humidity range of 36 RH% – 98 RH%.

Materials and Method

Preparation of Magnesium-Zinc Ferrite

In the present work, the cubic form of $Mg_{1-x}Zn_xFe_2O_4$ (where $x = 0.50$) was prepared by flash-combustion technique. The raw materials used in this preparation were Magnesium Nitrate Hexahydrate [$Mg(NO_3)_2 \cdot 6H_2O$], Zinc Nitrate Hexahydrate [$Zn(NO_3)_2 \cdot 6H_2O$] and Ferric Nitrate Nonahydrate [$Fe(NO_3)_3 \cdot 9H_2O$]. Urea [$CO(NH_2)_2$] was used as the fuel. De-ionized (DI) water was used as the solvent. According to the desired stoichiometric proportion, the pure nitrate solutions were weighed and mixed. Urea was added to the mixture (as fuel). The mixture was heated at $100^\circ C$. The mixture reacted leading to combustion and the reaction was complete in 30 min. A foamy and highly porous precursor mass was obtained. The ferrite precursor was dried at room temperature for 24 h and the dried powder was heated at $900^\circ C$ for 4 h for ferrite crystalline formation. The heat treatment of the precursor solution was performed in vacuum chamber (160 mmHg) by using

DELTA A Series Temperature Controller DTA4896. The K-type thermocouple was used as the temperature sensor to read-out the real temperature of the sample in the chamber. The desired as-prepared Mg-Zn mixed ferrite, $\text{Mg}_{0.5}\text{Zn}_{0.5}\text{Fe}_2\text{O}_4$ was obtained. Flow diagram of the sample preparation procedure is shown in Figure 1. Photographs of the starting materials, solutions of starting materials, precursor solutions, DELTA A Series Temperature Controller DTA4896 and experimental setup of sample preparation system are shown in Figures 2(a –f).

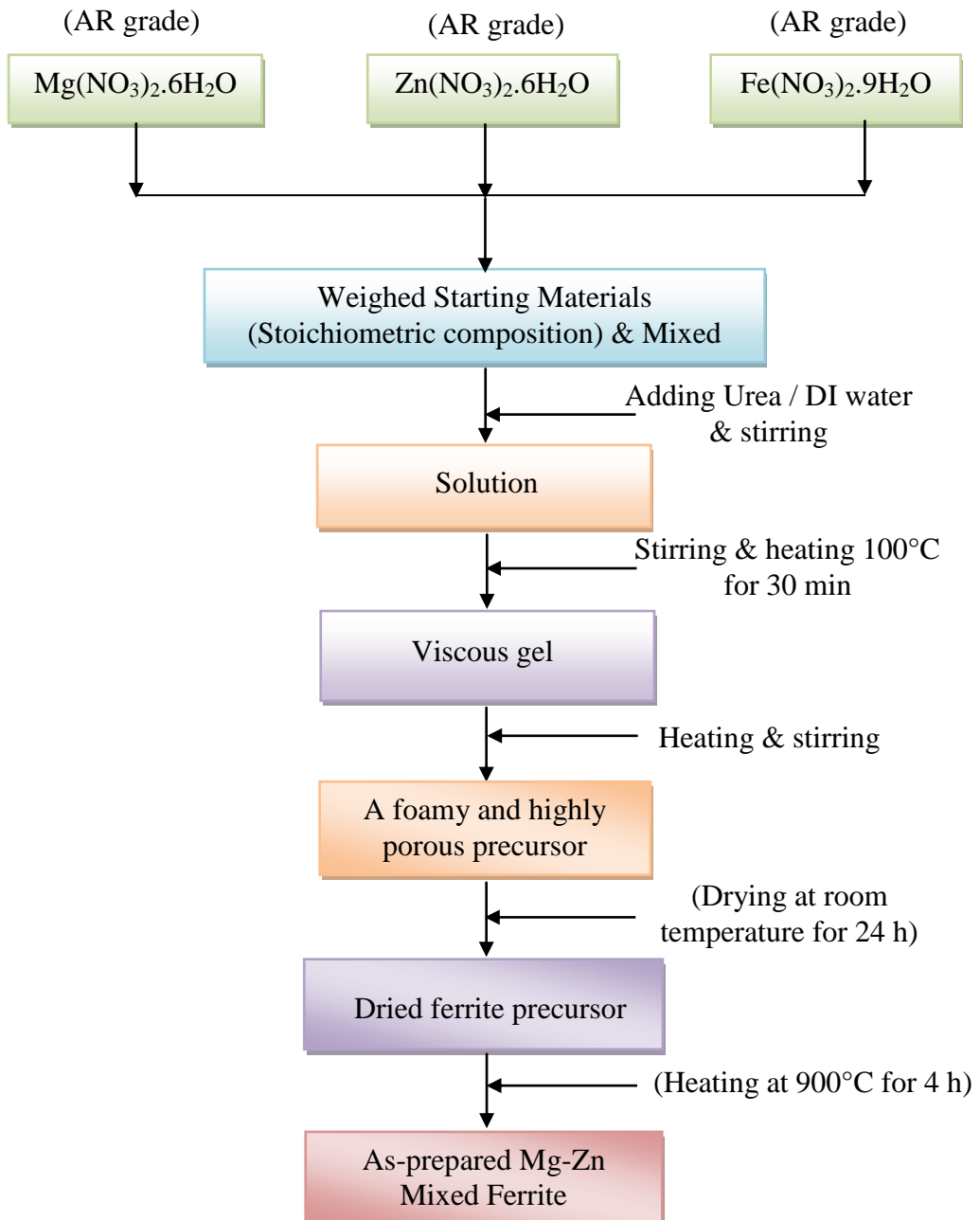


Figure 1: Flow diagram of the sample preparation procedure of $\text{Mg}_{0.5}\text{Zn}_{0.5}\text{Fe}_2\text{O}_4$ ferrite

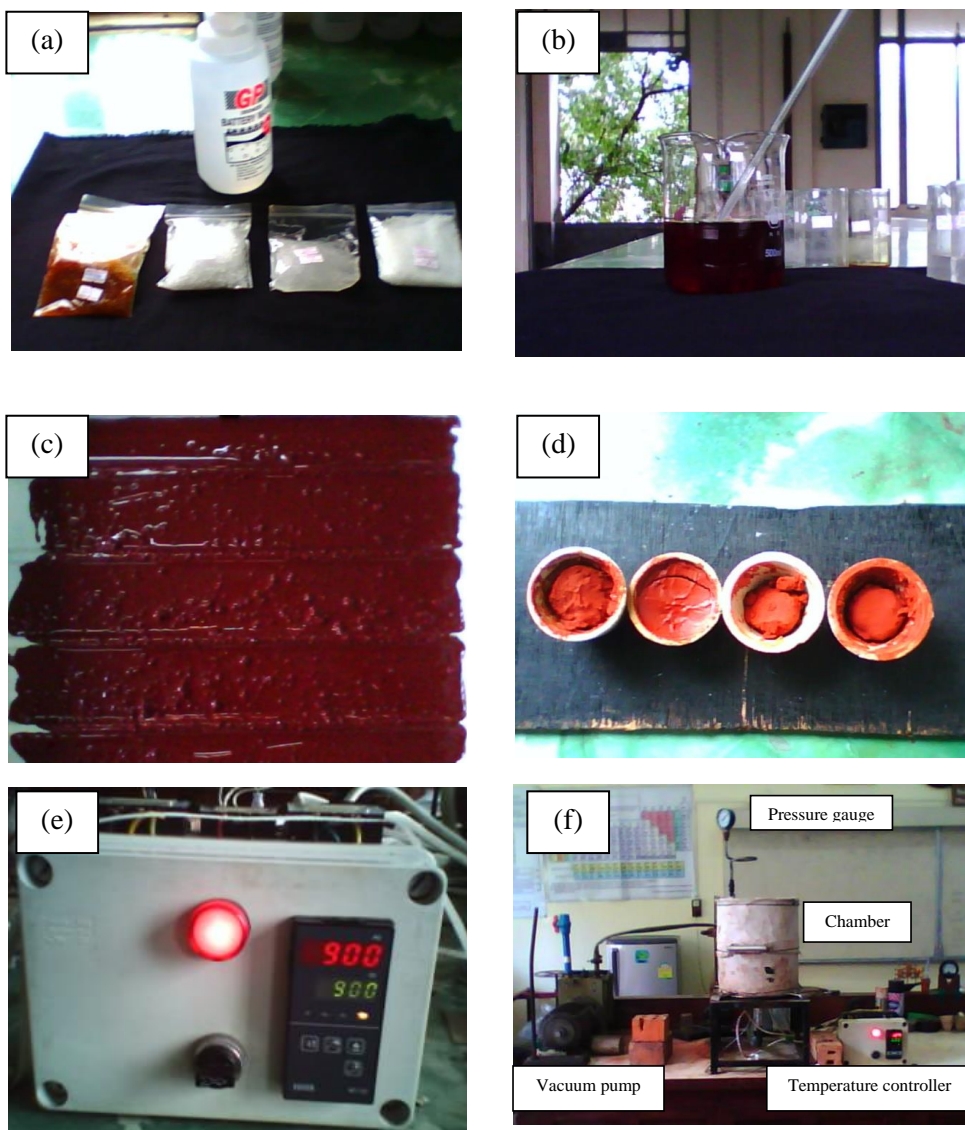


Figure 2: Photographs of the (a) weighed starting materials and DI water, (b) mixed solution, (c) foamy and highly porous precursor, (d) dried ferrite precursor, (e) DELTA A Series DTA4896 temperature controller and (f) experimental setup of sample preparation system

XRD, SEM and FTIR Measurements

Powder XRD pattern of the sample was investigated by RIGAKU MULTIFLEX X-Ray Powder Diffractometer. The X-ray diffractometry is mainly used for the identification and qualification of compounds by their diffraction patterns. SEM micrograph of the sample were observed by using JEOL JSM-5610LV SEM with the accelerating voltage of 15 kV, the beam current of 50 mA and 5500 times of photo magnification. FTIR transmission spectrum of the sample was recorded on PC-controlled SHIMADZU FTIR-8400 Spectrophotometer with Potassium Bromide, KBr, pellet method.

Temperature Dependent Electrical Resistance and Humidity Sensitive Electrical Properties Measurements

The sample was made into pellet by SPECAC hydraulic pellet-maker using 5 ton (~70 MPa). The silver paste was made over the sample to ensure good electrical contacts. The electrical resistance and capacitance of the sample were observed by FLUKE 45 DUAL DISPLAY MULTIMETER and FUKU DM6013A CAPACITANCE METER in the temperature range of 299 K – 773 K. CAHO SR-T903 Temperature Controller and K-type thermocouple were used as Temperature Controller and Temperature Sensor. 300 W heater rod was used as the heating element. The electrical conductivity

σ and dielectric constant ϵ_r of the sample were evaluated by using $\sigma = \frac{l}{RA}$

and $\epsilon_r = \frac{Cl}{\epsilon_0 A}$ where l is the distance between two electrodes, A is the cross-

sectional area of the electrodes, R is the resistance, C is the capacitance, and ϵ_0 is the permittivity of free space (8.8541×10^{-12} F m⁻¹). Photograph of the experimental setup of electrical conductivity measurement is shown in Figure 3. The dimensions of the sample are 1.14×10^{-4} m² in diameter and 3.83×10^{-3} m in thickness.

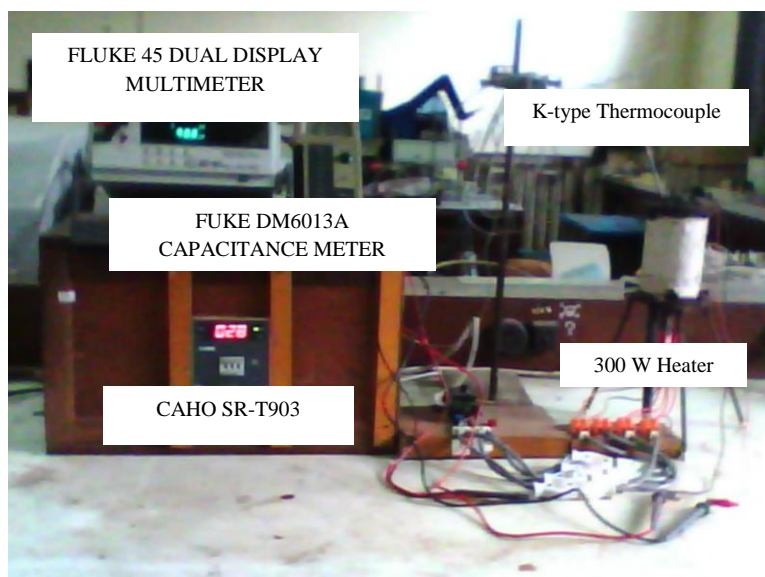


Figure 3: Photograph of the experimental setup for the temperature dependent resistance and capacitance measurement

Humidity-sensitive electrical properties of the sample were investigated in the increasing and decreasing relative humidity ranges 36 RH% – 98 RH% and 98 – 36 RH% for the application of humidity sensor. Area and thickness of the pellet were $1.14 \times 10^{-4} \text{ m}^2$ and $2.37 \times 10^{-3} \text{ m}$. Electrical resistance, dc voltage and capacitance of the sample were observed. In this measurement, Oktimer TDK0302LA Humidity Meter was used as the humidity sensing element. UNI-T UT802 digital multimeter was used as the digital resistance meter, voltmeter and capacitance meter. The refrigerator (TOSHIBA) was used as the humidity generator. Photograph of the experimental setup of humidity sensitive electrical property measurement are shown in Figure 4.

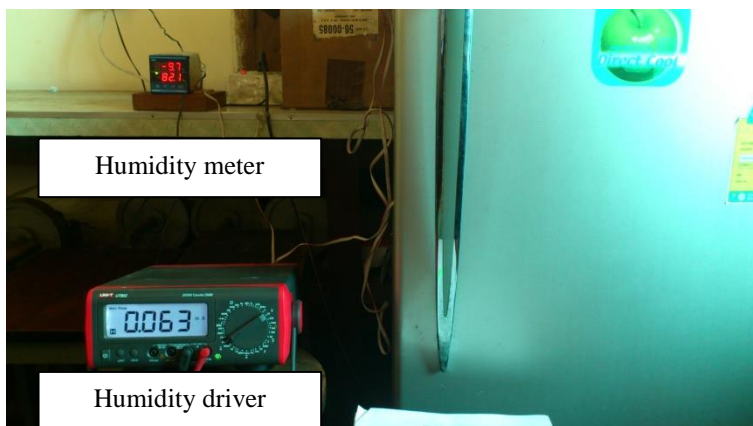


Figure 4: Photograph of the experimental setup of humidity sensitive electrical properties measurement

Results and Discussion

XRD Study

XRD pattern of Magnesium-Zinc ferrite, $Mg_{1-x}Zn_xFe_2O_4$ (where $x = 0.50$) is shown in Figure 5. The observed XRD lines were identified by using standard JCPDS data library files of (i) Cat. No. 88-1936 > Magnesioferrite, syn – $MgFe_2O_4$ and (ii) Cat. No. 73-1963 > $ZnFe_2O_4$ – Zinc Iron Oxide. The observed XRD data of diffraction angle ($^\circ$), atomic spacing (\AA), miller indices (hkl), Full Width at Half Maximum ($^\circ$) and peak height (%) of the sample are tabulated in Table 1. The appearance of the diffraction lines in the observed XRD patterns shows that the investigated sample is a single phase Magnesium-Zinc ferrite, $Mg_{1-x}Zn_xFe_2O_4$ (where $x = 0.50$) with spinel structure.

The diffraction line at 35.68° or (311) plane indicated that the crystallites were preferentially

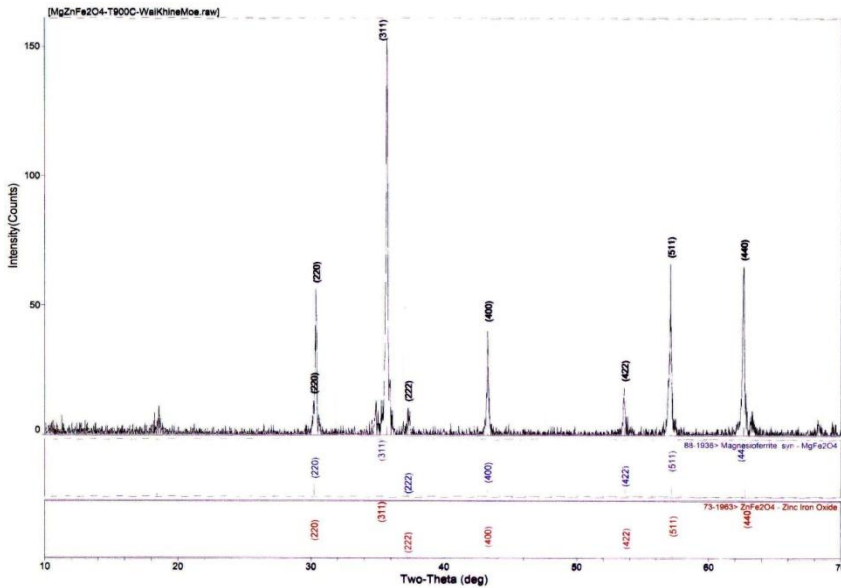


Figure 5: XRD pattern of $Mg_{1-x}Zn_xFe_2O_4$ (where $x = 0.50$)

oriented along (311) plane. The lattice parameters are evaluated by using crystal utility of the equation of $\frac{\sin^2 \theta}{(h^2 + k^2 + l^2)} = \frac{\lambda^2}{4a^2}$ where θ is the diffraction

angle ($^\circ$), (hkl) is the miller indices, λ is the wavelength of incident X-ray (\AA) and a is the lattice parameter of the samples (\AA). The obtained lattice parameters and the unit cell volume of the sample are obtained as $a = b = c = 8.3512 \text{\AA}$ and $582.43 (\text{\AA})^3$ respectively. Khot, S. S.et. al. (2011) has reported that the lattice parameters of the $Mg_{0.5}Zn_{0.5}Fe_2O_4$ ferrite prepared by co-precipitation method are 8.3560\AA . Thus, the obtained lattice parameters in the present study are found to be agreed with the results of Khot, S. S.et.al..

The broad peaks in the XRD patterns indicate a fine particle nature of the materials. In the present work, the particle size of Mg-Zn ferrite sample was calculated by using Scherrer's formula: $D = \frac{0.9\lambda}{B \cos \theta}$, where D is the

crystallite size (nm), λ is the wavelength (\AA), θ is the diffraction angle of the peak under consideration at FWHM ($^\circ$) and B is the observed FWHM (radians). The crystallite size of the sample is obtained as 47.96 nm by using

the strongest diffraction line of (311) plane. The result shows that the sample is an anisotropic material.

Table 4.1: XRD data of $Mg_{0.5}Zn_{0.5}Fe_2O_4$ ferrite

Line No	2θ (°)	(hkl)	$d(\text{Å})$	FWHM (°)	Height (%)
1 [#]	30.19	(220)	2.96	0.187	8.50
2 [*]	30.36	(220)	2.94	0.156	36.60
3 [*]	35.68	(311)	2.51	0.174	100.00
4 [*]	37.27	(222)	2.41	0.213	6.50
5 [#]	43.27	(400)	2.09	0.136	26.80
6 [*]	53.58	(422)	1.71	0.176	11.80
7 [*]	57.06	(511)	1.61	0.164	43.10
8 [*]	62.62	(440)	1.48	0.191	42.50

$ZnFe_2O_4$, * $MgFe_2O_4$

SEM Investigation

Figure 6 shows the SEM micrograph of as-prepared sample. As shown in figure, the grain shape sample is spherical and the sizes are obtained in the range of 0.20 μm – 0.50 μm . Also, the image shows that the $Mg_{0.5}Zn_{0.5}Fe_2O_4$ sample composed of agglomerated particles with poor grain boundary.

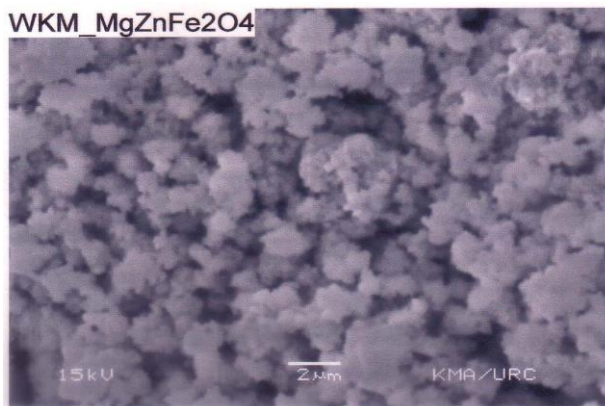


Figure 6: SEM micrograph of $Mg_{1-x}Zn_xFe_2O_4$ (where $x = 0.50$)

FTIR Analysis

The vibrational wavenumbers of pure MgFe_2O_4 are mainly 565 cm^{-1} and 581 cm^{-1} for A atoms on tetrahedral sites (ν_1 -mode) and 406 cm^{-1} and 433 cm^{-1} for B atoms on octahedral sites (ν_2 -mode). Also, vibrational frequencies of pure Zinc Ferrite, ZnFe_2O_4 , are mainly 550 cm^{-1} and 555 cm^{-1} for A atoms on tetrahedral sites (ν_1 -mode) and 415 cm^{-1} for B atoms on octahedral sites (ν_2 -mode).

FTIR transmission spectrum of the sample is shown in Figure 7. As shown in observed FTIR spectrum, four absorption lines are mainly observed and these lines are represented by the vibrational characteristics of as-prepared $\text{Mg}_{0.5}\text{Zn}_{0.5}\text{Fe}_2\text{O}_4$. The lines at the wavenumber 417 cm^{-1} and 448 cm^{-1} indicate the B atoms on octahedral sites and assigned as ν_2 -mode. The lines at 556 cm^{-1} and 586 cm^{-1} represent the vibrational characteristic of A atoms on tetrahedral sites and assigned as ν_1 -mode. The appearances of the collected lines represent the vibrational characteristics of as-prepared $\text{Mg}_{0.5}\text{Zn}_{0.5}\text{Fe}_2\text{O}_4$ material in which others lines, e.g., starting materials and solvent, not appeared.

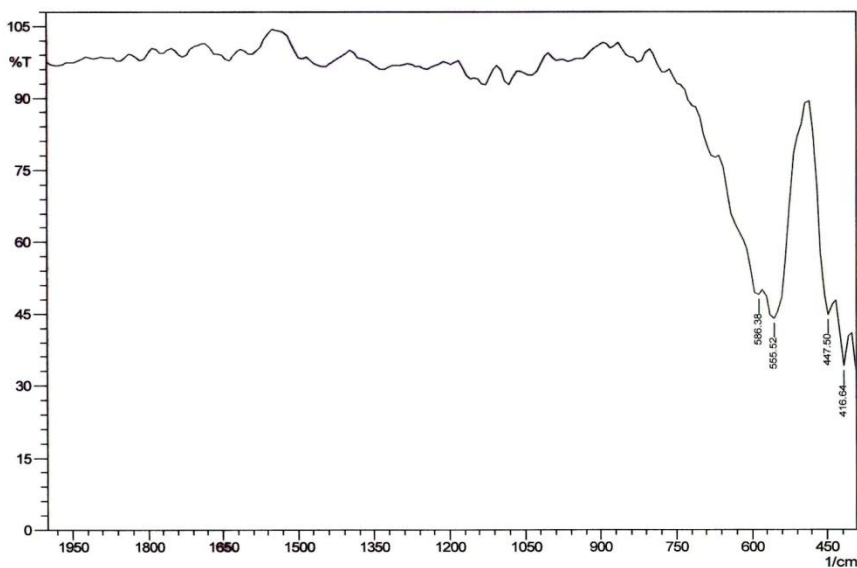


Figure 7: FTIR transmission spectrum of $\text{Mg}_{1-x}\text{Zn}_x\text{Fe}_2\text{O}_4$ (where $x = 0.50$)

Temperature Dependent Electrical Properties Study

Electrical properties of ferrites such as resistivity and conductivity generally depend upon the composition and preparation parameters of the synthesized materials. The electrical conductivity of a ferrite obeys an Arrhenius expression: $\sigma = \sigma_0 \exp(-E_a / kT)$, where σ is the conductivity, σ_0 is the pre-exponential factor, E_a is the activation energy for ionic conduction, k is the Boltzmann constant and T is the absolute temperature. The temperature dependence of d.c. electrical conductivity in the temperature range of 299 K – 773 K is shown in Figure 8. It is observed that the electrical conductivity of the sample increases with increase in temperature. The slope of the graph is fitted by linear regression method due to the analytical solving of Arrhenius expression and obtained as -4.4241. Then, the activation energy of the sample is evaluated as,

$$\frac{-E_a}{k} = -4.4241 \times 1000$$

$$E_a = 4.4241 \times 1000 \times 1.3806 \times 10^{-23}$$

$$E_a = 0.3818 \text{ eV}$$

The d.c. electrical conductivities are obtained as in the range of $3.8894 \times 10^{-8} \text{ S m}^{-1}$ (at 299 K) – $6.5607 \times 10^{-4} \text{ S m}^{-1}$ (at 773 K). It shows that the sample is a normal ionic conductor.

Plot of the variation of dielectric constant as a function of temperature of the sample in the temperature range 299 K – 773 K is shown in Figure 9. From the plot, dielectric constant increased with increase in temperature.

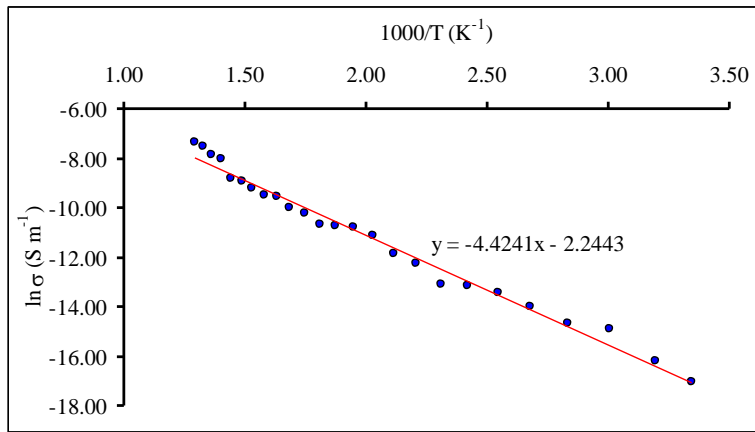


Figure 8: Temperature dependence of d.c. electrical conductivity of $Mg_{1-x}Zn_xFe_2O_4$ (where $x = 0.50$)

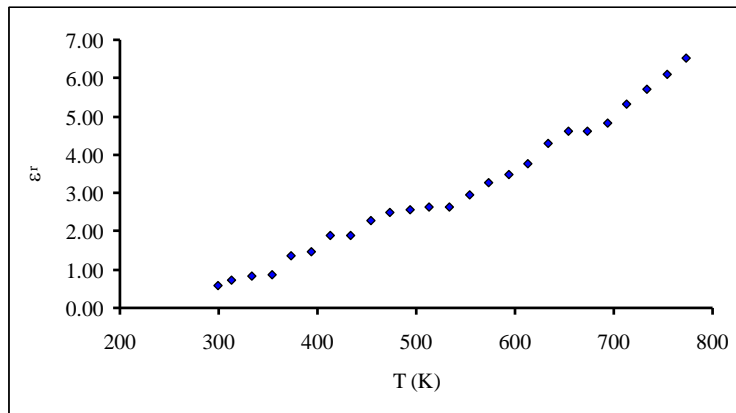


Figure 9: Temperature dependence of dielectric constant of $Mg_{1-x}Zn_xFe_2O_4$ (where $x = 0.50$)

Humidity Sensitive Electrical Properties Investigation

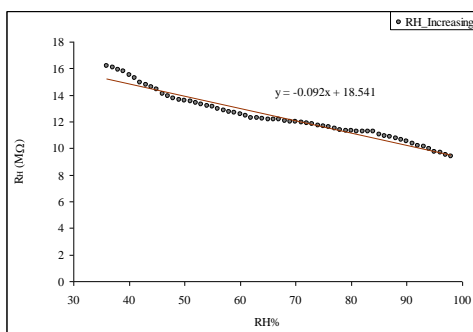
The electrical resistance, dc voltage and capacitance of the Magnesium-Zinc ferrite, $Mg_{0.5}Zn_{0.5}Fe_2O_4$, sample under investigation were measured in the relative humidity ranges of 36 RH% – 98 RH% and 98 RH% – 36 RH% with the step of 1 RH%. Variations of the humidity sensitive resistance, R_H , with relative humidity RH%, dc voltage, V_H , with relative humidity RH%, and capacitance, C_H , with relative humidity RH% of the

sample are shown in Figures 10(a – c) for the increasing humidity range of 36 RH% – 98 RH% and Figures 11(a – c) for the decreasing humidity range of 98 RH% – 36 RH%.

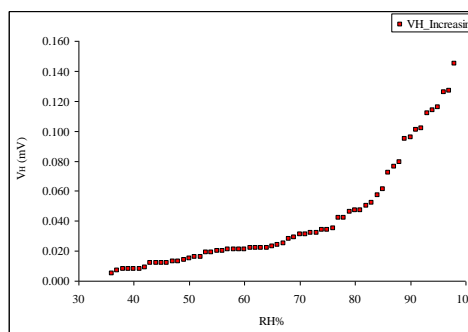
As shown in Figure 10(a) and Figure 11(a), the R_H vs RH% curves were fitted by linear type. The slopes of the sample were obtained as 0.092 $M\Omega/RH\%$ in 36 RH%– 98 RH% and 0.0483 $M\Omega/RH\%$ in 98 RH% – 36 RH% respectively. On inspection of figure, it was found that the resistance of the sample decreases with increase in humidity, as seen from slope of curve in Figure 10(a). Since, the sample can allow water molecules to pass through easily to reach the sensing surface, and can hold back condensation water from condensing directly on the surface of the sensing surface.

As presented in Figure 10(b) and Figure 11(b) of $V_H - RH\%$ graphs, under whole humidity ranges (36 RH% – 98 RH% and 98 RH% – 36 RH%), water adsorption on sample surface is likely the dominant factor for electrical conduction. Thus, the surface area would provide more sites for water adsorption and produce more charge carriers for electrical conduction.

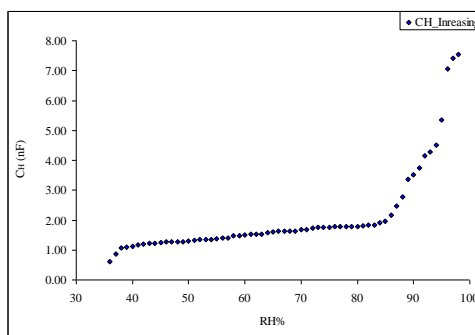
As shown in Figure 10(c) and Figure 11(c), the capacitance of the sample increases with increase in RH, it changes a little in about 40 RH% – 85 RH%, and changes greatly at high RH (85 RH% – 98 RH%). In 40 RH% – 85 RH% conditions, the resistance of the sample slightly decreased, but in high RH conditions it is greatly increased. It can be said that, as an electrolyte, the water molecule is not only physically absorbed in the active group of the copolymer, but also can be polarized. The effect can generate space charge and dipoles, and then accumulate and degenerate between electrodes. The result is the increase of capacitance with increasing RH. The sensitivity factor S_f of the sample was evaluated by using the equation and obtained as $S_f = R_{36 RH\%} / R_{98 RH\%} = 1.72$.



(a)

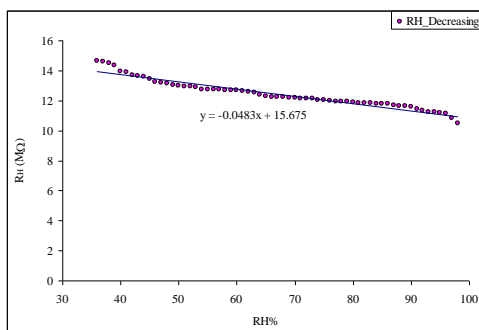


(b)

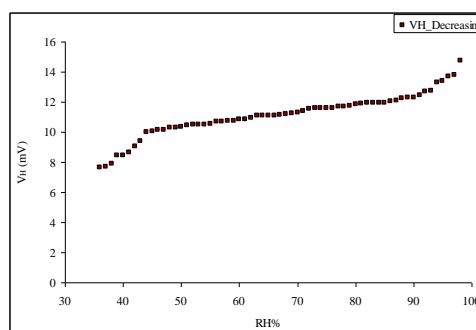


(c)

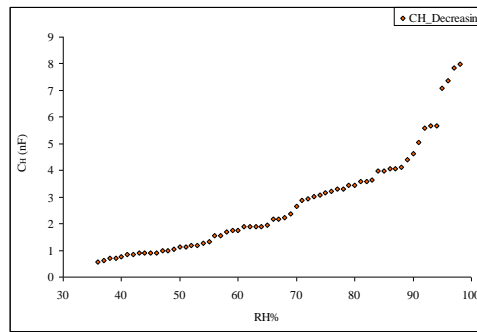
Figure10: Plots of the variations of (a) resistance R_H , (b) dc voltage V_H and (c) capacitance C_H with relative humidity RH% of $Mg_{1-x}Zn_xFe_2O_4$ (where $x = 0.50$) in increasing humidity range of 36 RH% – 98 RH%



(a)



(b)



(c)

Figure11: Plots of the variations of (a) resistance R_H , (b) dc voltage V_H and (c) capacitance C_H with relative humidity RH% of $Mg_{1-x}Zn_xFe_2O_4$ (where $x = 0.50$) in decreasing humidity range of 98RH% – 36 RH%

Conclusion

Nanosized Magnesium-Zinc ferrite, $Mg_{1-x}Zn_xFe_2O_4$ (where $x = 0.50$) was successfully prepared by flash-combustion technique. XRD pattern indicates that the sample is single phase cubic spinel structure with the lattice parameters $a = b = c = 8.3512 \text{ \AA}$. The crystallite size of the sample is obtained as 47.96 nm. From the SEM micrograph, the grain shape is spherical and the sizes are obtained as in the range of $0.20 \mu\text{m} - 0.50 \mu\text{m}$. From the FTIR spectrum, the bands observed in the wavenumber ranges of $420 \text{ cm}^{-1} - 480 \text{ cm}^{-1}$ and $520 \text{ cm}^{-1} - 590 \text{ cm}^{-1}$ correspond to octahedral and tetrahedral sites molecules. The electrical conductivity and dielectric constant of the sample increase with increase in temperature. The sample exhibits the normal ionic conductor with the activation energy 0.3818 eV. Humidity sensitive electrical resistance decrease with increase in humidity and the dc voltage and capacitance increase with increase in humidity. The sensitivity factor S_f of the sample was obtained as 1.72. According to experimental results, the sample can be used as humidity sensing materials due to its sensitivity and sensitivity factor are comparable with the ferrite humidity sensor.

Acknowledgement

The authors would like to acknowledge Professor Dr Khin Khin Win, Head Department of Physics, University of Yangon, for her valuable discussions and comments on this work.

References

- Bhattacharjee, K., Ghosh, C.K., MITRA, M.K. & DAS, G.C. (2011). Novel synthesis of $Ni_xZn_{1-x}Fe_2O_4$ ($0 \leq x \leq 1$) nanoparticles and their dielectric properties. *Journal of Nanoparticles Research*, 13, pp. 739–750.
- Brito, V.L.O. (2010). EVALUATION OF A Ni-Zn FERRITE FOR USE IN TEMPERATURE SENSORS. *Progress in Electromagnetic Research Letters*, 13, pp. 103–112.
- Gadkari, A.B., Shinde, T.J. & Vasambekar, P.N. (2013) Liquid petroleum gas sensor based on nanocrystallite $Mg_{0.6}Cd_{0.4}Fe_2O_4$. *Advanced Materials Letters*, 4(7), pp. 573–576.
- Maria1, K.H., Choudhury, S. & Hakim, M.A. (2013) Structural phase transformation and hysteresis behavior of Cu-Zn ferrites. Khot, S. S. & Watawe, S. C. (2011). EFFECT OF TEMPERATURE OF SYNTHESIS ON X-RAY, IR PROPERTIES OF MG-ZN FERRITES PREPARED BY OXALATE CO-PRECIPITATION METHOD. *International Journal of Advances in Engineering & Technology*, 1(4), pp. 422 – 429.
- International Nano Letters*, 3, pp. 1–10.
- Vagolu, V.K. & Samatha, K. (2013) Studies on Structural and Electrical Properties of Cobalt Substituted Nickel-Zinc Ferrites Prepared from Soft Chemical Method. *International Journal of Innovative Research and Studies*, 2(8), pp. 99–113.